Plant Physiology Preview. Published on April 28, 2017, as DOI:10.1104/pp.17.00475

Short Title: *DCLs* and siRNAs in Intra- and Intercellular VIGS

Corresponding Author: Yiguo Hong
Research Centre for Plant RNA Signaling, College of Life and Environmental Sciences, Hangzhou Normal University, Hangzhou 310036, China and Warwick-Hangzhou RNA Signaling Joint Laboratory, School of Life Sciences, University of Warwick, Coventry CV4 7AL, UK.

Telephone: +86-571-28866065
Fax: +86-571-28866065
E-mails: yiguo.hong@hznu.edu.cn; yiguo.hong@warwick.ac.uk

Primary Research Area: Virus-plant interactions/Cell Biology
2nd Research Area: Cell- and non-cell autonomous VIGS/Signaling and Response

15 Roles of Dicer-Like proteins 2 and 4 in Intra- and Intercellular Antiviral Silencing[1]

16

17 Cheng Qin[2], Bin Li[2], Yaya Fan[2], Xian Zhang[2], Zhiming Yu[2], Eugene Ryabov, Mei Zhao,
18 Hui Wang, Nongnong Shi, Pengcheng Zhang, Stephen Jackson, Mahmut Tör, Qi Cheng,
19 Yule Liu, Philippe Gallusci, and Yiguo Hong[*]

20

21 Research Centre for Plant RNA Signaling, College of Life and Environmental Sciences,
22 Hangzhou Normal University, Hangzhou 310036, China (C.Q., B.L., Y.F., X.Z., Z.Y.,
23 E.R., M.Z., H.W., N.S., P.C., Y.H.); Warwick-Hangzhou RNA Signalling Joint
24 Laboratory, School of Life Sciences, University of Warwick, Warwick CV4 7AL, UK
25 (E.R., S.J., Y.H.); Institute of Science and the Environment, University of Worcester,
26 Worcester WR2 6AJ, UK (M.T.); Biotechnology Research Institute, Chinese Academy of
27 Agricultural Sciences, Beijing 100081, China (Q.C.); MOE Key Laboratory of
28 Bioinformatics, Centre for Plant Biology, School of Life Sciences, Tsinghua University,
29 Beijing 100084, China (Y.L.); l'UMR Ecophysiologie et Génomique Fonctionnelle de la
30 Vigne, ISVV, 210 Chemin de Leysotte, CS 50008, 33882 Villenave d'Ornon, France
31 (P.G.).

32

33 [1]**Funding:** This work was supported by grants from the National Natural Science
34 Foundation of China (NSFC, 31370180 to Y.H.), Ministry of Agriculture of the People's
35 Republic of China (the National Transgenic Program of China 2016ZX08009001-004 to
36 Y.H.); Hangzhou Normal University (Pandeng Program 201108 to Y.H.); the Hangzhou
37 City Government (Innovative Program for Science Excellence 20131028 to Y.H.); the
38 UK Biotechnology & Biological Sciences Research Council (UK-China Partnering
39 Award BB/K021079/1 to S.J. and Y.H.); the NSFC and Zhejiang Provincial Natural
40 Science Foundation (31500251 to C.Q., 31201490 to X.Z, 31200913 to Z.Y.,
41 LY15C14006 to X.Z. and LY14C010005 to N.S.).

42

43 [2]These authors contributed equally to this work.

44

Author Contributions: C.Q., B.L., Y.F., X.Z., and Z.Y. designed, performed experiments and analysed data; E.R. performed bioinformatics analysis. M.Z., H.W., N.S. and P.Z. performed research; S.J., M.T., Y.L. and Q.C. were involved in the analysis of data and helped writing the paper. Y.H. conceived and initiated the project, designed experiments, analysed data and wrote the paper.

One-sentence Summary: DCL4 inhibited intercellular VIGS whilst DCL2 along with DCL2-processed/dependent siRNAs were involved in non-cell autonomous VIRS in Nicotiana benthamiana.

[*]Address correspondence to yiguo.hong@hznu.edu.cn; yiguo.hong@warwick.ac.uk
The author responsible for distribution of materials integral to the findings presented in this article in accordance with the policy described in the instructions for Authors (www.plantphysioll.org) is: Yiguo Hong (yiguo.hong@hznu.edu.cn, yiguo.hong@warwick.ac.uk).

ABSTRACT

RNA silencing is an innate antiviral mechanism conserved in organisms across kingdoms. Such a cellular defence involves DICER or DICER-LIKEs (DCLs) that process plant virus RNAs into viral small interfering (vsi)RNAs. Plants encode four *DCLs* which play diverse roles in cell-autonomous intracellular virus-induced RNA silencing (known as VIGS) against viral invasion. VIGS can spread between cells. However, the genetic basis and involvement of vsiRNAs in non-cell autonomous intercellular VIGS remains poorly understood. Using GFP as a reporter gene together with a suite of *DCL* RNAi transgenic lines, here we show that despite the well-established activities of *DCLs* in intracellular VIGS and vsiRNA biogenesis, *DCL4* acts to inhibit intercellular VIGS whilst *DCL2* is required (likely along with DCL2-processed/dependent vsiRNAs and their precursor RNAs) for efficient intercellular VIGS trafficking from epidermal to adjacent cells. *DCL4* imposed an epistatic effect on *DCL2* to impede cell-to-cell spread of VIGS. Our results reveal previously unknown functions for *DCL2* and *DCL4* which may form a dual defensive frontline for intra- and intercellular silencing to double-protect cells from virus infection in *Nicotiana benthamiana*.

Keywords: DICER-LIKEs, vsiRNAs, non-cell autonomous intercellular VIGS, *Nicotiana benthamiana*

INTRODUCTION

RNA silencing targets endogenous cellular nucleic acids and exogenous invasive pathogenic RNAs or DNAs for homologous RNA-dependent degradation, translation repression or RNA-directed DNA methylation (RdDM) in eukaryotic organisms (Baulcombe, 2004; Sarkies and Miska, 2014). In plants, RNA silencing forms an innate defence against virus infection (Aliyari and Ding, 2009; Csorba et al., 2015). Such an antiviral mechanism involves DICER-LIKE (DCL) ribonuclease type III enzymes. Most plants encode four DCLs of which DCL1 is responsible for production of microRNA whilst DCL2, DCL3 and DCL4 are responsible for biogenesis of 22, 24 and 21nt small interfering RNA (siRNA), respectively (Mukherjee et al., 2013). DCL2 and DCL4 possess partially redundant functions in the production of trans-acting siRNA, but DCL2 acts predominantly to manufacture various sized secondary siRNAs (Chen et al., 2010; Henderson et al., 2006; Xie et al., 2005). Unlike animal viruses, plant viruses have not yet been found to encode any microRNA or specific site that can be targeted by host cellular microRNAs. However, artificial microRNAs can inhibit plant virus invasion (Qu et al., 2007). In *Arabidopsis*, DCLs can process plant virus RNAs into vsiRNAs within individual cells. For instance, *DCL4* and DCL4-processed 21nt vsiRNAs are involved in virus-induced RNA silencing (also known as VIGS), a kind of post-transcriptional gene silencing (PTGS; Bouche et al., 2006; Garcia-Ruiz et al., 2010; Qu et al., 2008). *DCL2* and its cognate 22nt vsiRNAs may also affect VIGS in plant cells when *DCL4* is absent or defective (Andika et al., 2015; Wang et al., 2011; Zhang et al., 2012). On the other hand, *DCL3* and 24nt vsiRNAs are associated with RdDM and transcriptional gene silencing (TGS) in the protection of plant cells from DNA virus infection (Aregger et al., 2012; Blevins et al., 2006). In *Arabidopsis*, *DCL4* and *DCL2* also play hierarchical and redundant roles in intracellular antiviral silencing (Bouche et al., 2006; Garcia-Ruiz et al., 2010; Wang et al., 2011). Recently, a combined activity of *DCL2* and *DCL3* has been reported to be critical in defending plants from viroid infection (Katsarou et al., 2016). DCL1 can negatively regulate DCL4-initiated antiviral RNA silencing pathway (Qu et al., 2008). However, the roles of the different *DCLs* in promoting intercellular VIGS for plant systemic acquired resistance to virus infection are unclear.

In response to virus infection, intracellular VIGS in the initial virus-infected cells triggers intercellular silencing in adjacent cells, which spreads systemically to remote tissues. This is known as non-cell autonomous VIGS. Non-cell autonomous VIGS combats incoming viruses and protects recipient cells from further viral invasion (Schwach et al., 2005). In *Arabidopsis*, spread of the phloem-originating PTGS from companion cells to nearby cells requires *DCL4* and DCL4-processed 21nt siRNA signals (Dunoyer et al., 2005). However, whether 21nt siRNAs represent the bona fide silencing signals that are transportable among plant cells is highly controversial (Berg, 2016). On the other hand, *DCL2* can stimulate transitive PTGS and biogenesis of secondary siRNAs (Mlotshwa et al., 2008). *DCL2* can also restore silencing in the *Arabidopsis dcl4* mutant that is deficient in cell-to-cell spread of transgene-mediated PTGS (Parent et al., 2015). Moreover, intercellular and systemic PTGS involve many cellular factors including RDR6 which has been shown to be required for efficient cell-to-cell movement of VIGS (Melnyk et al., 2011; Qin et al., 2012; Searle et al., 2010; Smith et al., 2007). Nonetheless, the genetic basis and requirement of vsiRNAs for cell-to-cell and systemic spread of antiviral VIGS remain to be elucidated.

We previously developed a Turnip crinkle virus (TCV)-based local silencing assay to investigate intra- and intercellular VIGS in *Nicotiana benthamiana* (Qin et al., 2012; Ryabov et al., 2004; Shi et al., 2009; Zhou et al., 2008). TCV belongs to *Carmovirus* with a single positive-stranded RNA genome (Carrington et al., 1989). It encodes five proteins, namely the RNA-dependent RNA polymerases P28 and its read-through P88, movement proteins P8 and P9 and coat protein (CP) P38 (Carrington et al., 1989; Hacker et al., 1992; Li et al., 1998). CP is a strong viral suppressor of RNA silencing (VSR; Chattopadhyay et al., 2015; Merai et al., 2006; Perez-Canamas et al., 2015; Qu et al., 2003; Thomas et al., 2003; Zhang et al., 2012). It is also required for cell-to-cell movement of TCV in *N. benthamiana* (Cohen et al., 2000; Li et al., 2009). TCV/GFPΔCP in which CP is replaced with the 714nt GFP sequence (dubbed *TcvGFP* hereafter) is movement-deficient. This movement-deficient virus is still infectious but the virus remains restricted to the infected cell (Ryabov et al., 2004). Cell-to-cell spread of TCV/GFPΔCP can be complemented by heterologous silencing suppressors (Shi et al., 2009). However in the absence of the strong VSR CP, the movement-deficient

TCV/GFPΔCP can initiate intracellular VIGS that efficiently spreads to neighbouring epidermal and mesophyll cells (Qin et al., 2012; Ryabov et al., 2004; Shi et al., 2009; Zhou et al., 2008). Using this intra- and intercellular VIGS assay together with a suite of transgenic *DCL* RNAi lines, we have examined how the different *DCLs* affect viral siRNA biogenesis, intra- and intercellular VIGS in *N. benthamiana*. Our findings lead us to propose a model where intra- and intercellular VIGS comprise two separate components of an integrated viral defence strategy in which *DCL2* and *DCL4* play different roles.

RESULTS

DCL RNAi Does Not Affect Cell-to-Cell Mobility of TCV/GFPΔCP

To dissect the genetic requirements and silencing signals involved in non-cell autonomous intercellular VIGS (Fig. 1) in *N. benthamiana* (*Nb*), we utilized a suite of *DCL* RNAi transgenic *Nb* lines including *DCL1i*; *DCL2Ai* and *DCL2Bi*; *DCL3Ai* and *DCL3Bi*; *DCL4Ai* and *DCL4Bi*; and one double RNAi line *DCL24i* (Supplemental Table S1). We also used *GFP* transgenic lines *16cGFP*; *GfpDCL1i*; and lines *Gfp*; *GfpDCL2Ai* and *GfpDCL2Bi*; *GfpDCL3Ai* and *GfpDCL3Bi*; *GfpDCL4Ai* and *GfpDCL4Bi*, which were derived from crosses between *16cGFP* and *Nb* or *DCL* RNAi lines, respectively, as well as a triple cross line *GfpDCL24i* (Supplemental Table S1). We performed qRT-PCR assays and revealed that *DCL2, DCL3* and *DCL4* transcript levels were down-regulated by 60-80% in each of the two independent RNAi lines; however only about 40% reduction was achieved for *DCL1* in *DCL1i* (Fig. 1A). We then analyzed the impact of *DCL* RNAi on cell-to-cell mobility of TCV/GFPΔCP (Fig. 1B-G). The upper epidermises of leaves in each *DCL* RNAi plant at the six-leaf stage were inoculated with TCV/GFPΔCP. As observed under the fluorescent microscope, strong GFP green fluorescence appeared only in single epidermal cells in leaves of the wild-type *Nb* control (Fig. 1C) and all *DCL* RNAi plants (Fig. 1D-G). These results demonstrate that presence of TCV/GFPΔCP was limited to individual virus-infected epidermal cell, and that *DCL* RNAi did not affect the movement-deficiency of TCV/GFPΔCP.

DCL4 RNAi Enhances, whilst *DCL2* RNAi Reduces, Cell-to-Cell Spread of VIGS

To test whether intra- and intercellular VIGS is affected by the down-regulation of individual *DCL* genes, we used GFP as a reporter and mechanically inoculated the movement-deficient TCV/GFPΔCP onto young leaves of *16cGFP* (Fig. 1H), *GfpDCL1i* (Fig. 1I), *Gfp* (Fig. 1J), *GfpDCL2Ai* and *GfpDCL2Bi* (Fig. 1K and L), *GfpDCL3Ai* and *GfpDCL3Bi* (Fig. 1M and N) and *GfpDCL4Ai* and *GfpDCL4Bi* (Fig. 1O and P) plants. We then counted the number of *GFP* silencing foci on both upper and lower epidermises of the inoculated leaves, and measured sizes in diameter of 80-560 randomly selected silencing foci on the upper epidermises (Fig. 1H-U; Supplemental Table S2). We used the number and size of silencing foci as well as the 'silencing cell-to-cell-spread index

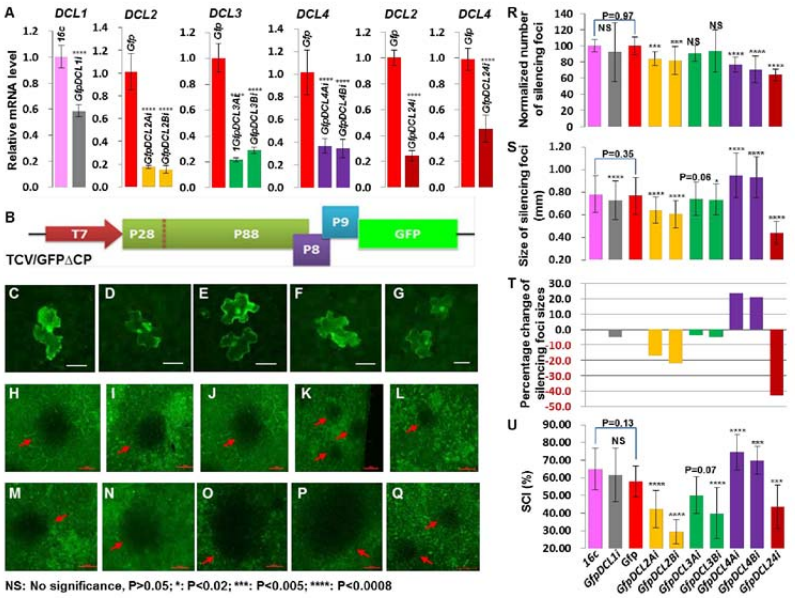

Figure 1. Different Roles of *DCLs* in the Cell-to-cell Spread of VIGS. (A) Down-regulation of *DCL* expression by RNAi. Young leaves were collected from *DCLi* plants at 7 days post-inoculation (dpi), and the level of *DCL* RNAs was analysed by qRT-PCR. (B) Schematic of the intracellular RNA silencing trigger TCV/GFPΔCP. The T7 promoter, viral RNA-dependent RNA polymerases (P28, P88), movement proteins (P8 and P9) and GFP are indicated. (C-G) Restricted localization of TCV/GFPΔCP in single epidermal cell of *Nb* (C), *DCL1i* (D) *DCL2Ai* (E), *DCL3Bi* (F) and *DCL4Ai* (G) plants. (H-Q) Intercellular *GFP* silencing foci (dark patches indicated by red arrows). Photographs of silencing foci on leaves of *16cGFP* (H); *GfpDCL1i* (I); *Gfp* (J); *GfpDCL2Ai* (K) and *GfpDCL2Bi* (L); *GFPDCL3Ai* (M) and *GfpDCL3Bi* (N); *GfpDCL4Ai* (O) and *GfpDCL4Bi* (P); and a triple-cross line *GfpDCL24i* (Q), were taken under a fluorescent microscope at 7 dpi. Bar=500μm. (R) Normalized number of *GFP* silencing foci per upper epidermis. Silencing foci were counted at 7 dpi from 3-21 different plant leaves inoculated with TCV/GFPΔCP. (S) and (T) Average size (diameters, S) and percentage change (T) of silencing foci. 80-560 silencing foci on different upper epidermises were randomly selected and measured. (U) SCI calculated as percentage of number of silencing foci on lower epidermis out of the number of silencing foci on upper epidermis. Student's ***t***-tests were performed for qRT-PCR and silencing data (mean ± standard deviation) and P-values are indicated (asterisks).

180 (dubbed SCI hereafter)' to assess the influence of *DCL* RNAi on intra- and intercellular
181 VIGS (Supplemental Text S1). Compared to *16cGFP* and *Gfp* controls (Fig. 1H and J),
182 *DCL2* RNAi caused 17-22% decrease in the average sizes of silencing foci (Fig. 1K, L, S
183 and T; Supplemental Table S2). SCI was reduced from approximately 58% in *Gfp* plants

to 29-42% in *GfpDCL2Ai* and *GfpDCL2Bi* plants (Fig. 1U; Supplemental Table S2). *DCL2* RNAi also caused a reduction in the number of silencing foci per leaf (Fig. 1R; Supplemental Table S2). RNAi knock-down of *DCL1* or *DCL3* did not affect the number of silencing foci and only reduced cell-to-cell movement of VIGS to a small extent, as evidenced by 3-5% decreases in silencing foci sizes and/or some reductions in SCI (Fig. 1H-J, M, N and R-U; Supplemental Table S2). This suggests that *DCL3* and/or *DCL1* may not contribute significantly to intercellular VIGS. A possible role cannot be ruled out completely, however, due to discrepancy between the two *GfpDCL3i* lines, and for we only have data from a single *GfpDCL1i* line. As with *DCL2* RNAi, *DCL4* RNAi caused a reduction in the number of silencing foci in *GfpDCL4Ai* and *GfpDCL4Bi* plants (Fig. 1R; Supplemental Table S2). This is consistent with the predominant role that *DCL4* plays in intracellular VIGS. To our surprise, the average sizes of silencing foci increased by more than 20% (Fig. 1O, P, S and T; Supplemental Table S2). The SCI also raised from around 58% in the *Gfp* controls to 70-75% in the two *GfpDCL4* RNAi lines (Fig. 1U; Supplemental Table S2). These results demonstrate that *DCL4* RNAi reduced intracellular silencing, but enhanced intercellular spread of VIGS. Taken together, our findings show that *DCL4* RNAi enhances but *DCL2* RNAi reduces cell-to-cell spread of VIGS in *Nb*.

DCL4 Interferes With _DCL2_ to Control Intercellular VIGS

To investigate whether *DCL4* and *DCL2* would affect each other to influence cell-to-cell spread of VIGS in *Nb*, we inoculated the triple-cross *GfpDCL24i* plant with TCV/GFPΔCP. We found a marked reduction in the number of *GFP* silencing foci (Fig. 1R; Supplemental Table S2), consistent with the reduction in the number of silencing foci observed in *GfpDCL2* RNAi and *GfpDCL4* RNAi lines. However, in the triple-cross plants, the average sizes of silencing foci decreased by more than 40%, and SCI also fell from 58% to 44% when compared to the *Gfp* control (Fig. 1Q, S-T; Supplemental Table S2). These results demonstrate that simultaneous RNAi of both *DCL2* and *DCL4* reduced both intra- and intercellular VIGS, similar to what is seen in *GfpDCL2* RNAi lines but to a greater extent. The inhibition of intercellular spread of VIGS in the triple-cross *GfpDCL24i* line is opposite to the increase in intercellular VIGS seen in the *GfpDCL4*

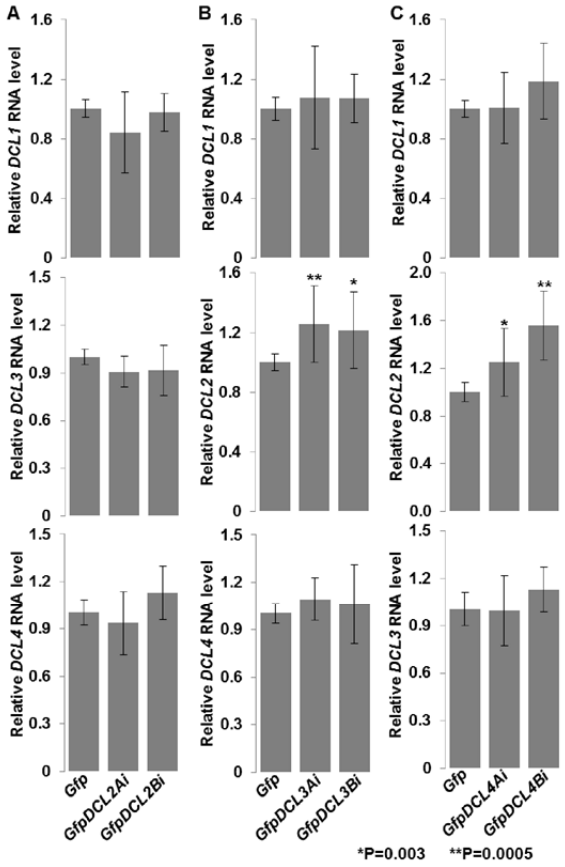

Figure 2. Regulation of *DCL2* Expression by *DCL3* and *DCL4*. (A-C) Effects of RNAi of *DCL2* (A), *DCL3* (B) and *DCL4* (C) on *DCL* gene expression. Young leaf tissues were collected at 6-8 leaf stage from four different plants of each transgenic line as indicated. RNA transcripts were analysed by qRT-PCR. Four technical replicates for qRT-PCR assays were performed on each cDNA of four biological duplicates (n = 4; leaf tissues from four different transgenic plants). Student's *t*-tests were performed for data (mean ± standard deviation) and P-values are indicated (asterisks). *DCL2i* does not affect expression of *DCL1*, *DCL3* or *DCL4* (A). However *DCL3i* (B) or *DCL4i* (C) resulted in increased mRNA levels of *DCL2*.

215 RNAi lines. This implies that *DCL4* imposed an epistatic effect on *DCL2* to affect
216 intercellular VIGS. This conclusion is supported by data from qRT-PCR assays (Fig. 2).
217 *DCL2* RNAi had no obvious impact on mRNA levels of *DCL1*, *DCL3* and *DCL4* (Fig.
218 2A). However, *DCL4* RNAi led to a 20–40% increase in *DCL2* expression but had no

substantial influence on the transcript levels of *DCL1* or *DCL3*; *DCL3* RNAi also enhanced the level of *DCL2* transcripts, but did not affect expression of *DCL1* or *DCL4* (Fig. 2B, C). Together with the specific RNAi effects on each *DCL* (Supplemental Dataset S1), these data reveal that *DCL4* is involved in a negative regulation of *DCL2* expression and as a consequence affecting the intercellular spread of VIGS in *Nb*.

DCLs Play Differential Roles in vsiRNA Biogenesis

To further understand how *DCLs* contribute to intra- and intercellular VIGS, we performed next generation sequencing of sRNA libraries for mock- or TCV/GFPΔCP-inoculated *Gfp*, *GfpDCL1i*, *GfpDCL2Ai*, *GfpDCL3Bi* and *GfpDCL4Ai* (Supplemental Text S2; Supplemental Dataset S1-3; Supplemental Fig. S1). We then mapped vsiRNAs and *TcvGFP* siRNAs onto the sequence of TCV/GFPΔCP (Fig. 3; Supplemental Fig. S2) and TCVΔCP (Supplemental Fig. S3-4). We found abundant vsiRNAs in TCV/GFPΔCP-inoculated RNAi lines (Fig. 3A-E; Supplemental Fig. S3A-E), compared to their mock controls (Supplemental Fig. S2A-E; Supplemental Fig. S4A-E; Supplemental Table S3). This is consistent with induction of effective VIGS in these plants (Fig. 1H-U; Supplemental Table S2). More vsiRNAs were recorded in *GfpDCL1i*, *GfpDCL2Ai* and *GfpDCL3Bi* plants (Fig. 3B-D; Supplemental Fig. S3B-D) than in *Gfp* controls (Fig. 3A; Supplemental Fig. S3A; Supplemental Table S3). However, the reads of vsiRNAs, particularly in the sense polarity, decreased in *GfpDCL4Ai* plants (Fig. 3E; Supplemental Fig. S3E; Supplemental Table S3) despite a marked increase in the overall number of siRNAs (vsiRNAs and *TcvGFP*-siRNAs) mapped to TCV/GFPΔCP (Supplemental Table S3). These results are consistent with the reduced level of recombinant viral RNAs in TCV/GFPΔCP-inoculated *DCL* RNAi plants, compared to the non-RNAi controls (Supplemental Fig. S5). On the other hand, the distribution of vsiRNAs across TCV/GFPΔCP (Fig. 3A-E) or TCVΔCP (Supplemental Fig. S3A-E) was identical among all virus-inoculated RNAi and control plants. Taken together, these data demonstrate that *DCL4* is able to efficiently target viral RNAs for the production of vsiRNAs during cell-autonomous VIGS. Our results also reveal that *DCL2* is required for cell-to-cell spread of VIGS, and *DCL2* could target viral RNA and *TcvGFP* mRNA for degradation in *Nb*.

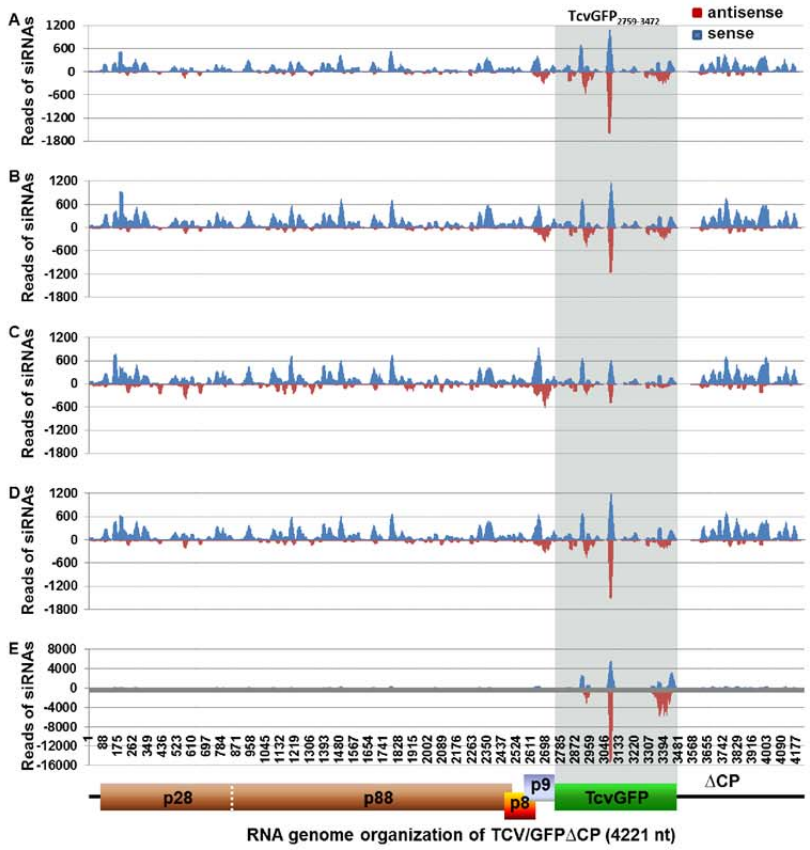

Figure 3. Distribution of 20-25nt vsiRNAs and siRNA$_{TcvGFP}$ across the TCV/GFPΔCP RNA. (A) *Gfp*. (B) *GfpDCL1i*. (C) *GfpDCL2Ai*. (D) *GfpDCL3Bi*. (E) *GfpDCL4Ai*. The sRNA libraries were generated from sRNA samples extracted from TCV/GFPΔCP-inoculated leaves. Blue and red bars represent siRNAs aligned to the sense (positive) and antisense (negative) strands of TCV/GFPΔCP viral RNA and *TcvGFP* mRNA (highlighted), respectively. The TCV/GFPΔCP genome organisation is indicated.

Antagonistic Influences of *DCL4* and *DCL2* on Accumulation of siRNAs Associated with Intercellular VIGS

In contrast to the situation with vsiRNAs, *GfpDCL* RNAi lines differed in the generation of *TcvGFP* or transgene *16cGFP* siRNAs (dubbed siRNA$_{TcvGFP}$ and siRNA$_{16cGFP}$) that are

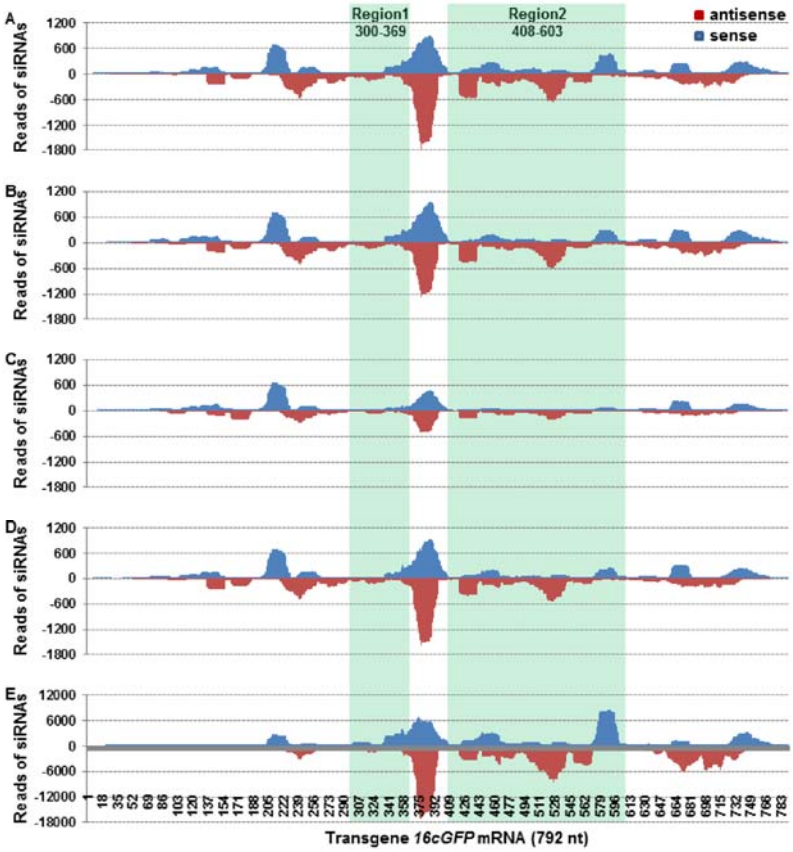

Figure 5. Distribution of 20-25nt *GFP* siRNAs across the 792nt Transgene *16cGFP* mRNA. (A) *Gfp*. (B) *GfpDCL1i*. (C) *GfpDCL2Ai*. (D) *GfpDCL3Bi*. (E) *GfpDCL4Ai*. The sRNA libraries were generated from sRNA samples extracted from TCV/GFPΔCP-inoculated leaves. Blue and red bars represent siRNAs aligned to the sense (positive) and antisense (negative) strands of *16cGFP* mRNA, respectively. The two regions (Region 1 and Region 2) having less sequence similarity with that of the transgene *TcvGFP* mRNA (see Fig. 4) as well as nucleotide coordinates are indicated.

254 associated with intra- and intercellular VIGS. Note that the 714nt *TcvGFP* (Ryabov et al.,
255 2004) and 792nt *16cGFP* (Haseloff et al., 1997; Ruiz et al., 1998) mRNAs are not
256 identical. Sequences between nucleotides 237-306 and 345-540 in *TcvGFP* (designated
257 $TcvGFP_{237\text{-}306}$ and $TcvGFP_{345\text{-}540}$) differ from the corresponding regions 300-369 and

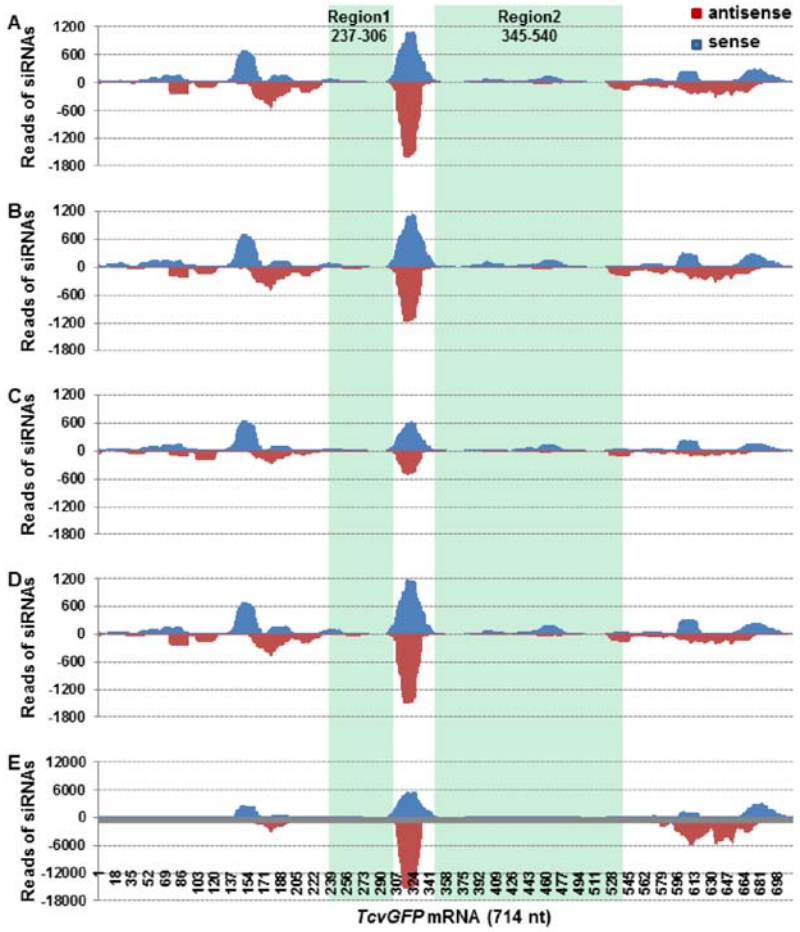

Figure 4. Distribution of 20-25nt *GFP* siRNAs across the 714nt *TcvGFP* mRNA. (A) *Gfp*. (B) *GfpDCL1i*. (C) *GfpDCL2Ai*. (D) *GfpDCL3Bi*. (E) *GfpDCL4Ai*. The sRNA libraries were generated from sRNA samples extracted from TCV/GFPΔCP-inoculated leaves. Blue and red bars represent siRNAs aligned to the sense (positive) and antisense (negative) strands of *TcvGFP* mRNA, respectively. The two regions (Region 1 and Region 2) having less sequence similarity with that of the transgene *16cGFP* mRNA (see Fig. 5) as well as nucleotide coordinates are indicated.

408-603 in *16cGFP* (designated $16cGFP_{300-369}$ and $16cGFP_{408-603}$) (Supplemental Fig. S6). Compared to the *Gfp* control and *GfpDCL1i* and *GfpDCL3Bi* plants, the levels of $siRNA_{TcvGFP}$ and $siRNA_{16cGFP}$ were reduced in *GfpDCL2Ai*, but significantly increased in *GfpDCL4Ai* (Supplemental Table S3). We then mapped the siRNAs onto *TcvGFP* (Fig. 4;

Supplemental Fig. S7) and *16cGFP* mRNA (Fig. 5; Supplemental Fig. S8). The distribution of sense and antisense *GFP* siRNAs to regions that are identical in *TcvGFP* and *16cGFP* was essentially the same in *Gfp* and in each of the *DCL* RNAi lines, however, the levels of siRNA$_{TcvGFP}$ and siRNA$_{16cGFP}$ were lower in *GfpDCL2Ai*, and much higher in *GfpDCL4Ai*, compared to *Gfp*, *GfpDCL1i* and *GfpDCL3Bi* (Fig. 4A-E; Fig. 5A-E; Supplemental Table S3). Moreover in *GfpDCL4Ai* the level of siRNA$_{16cGFP}$ (2.5 million reads) was approximately double compared to the abundance of siRNA$_{TcvGFP}$ (1.28 million reads) (Supplemental Table S3). Such substantial differences between siRNA$_{TcvGFP}$ and siRNA$_{16cGFP}$ levels suggest that the transgene *16cGFP* mRNA was targeted and diced by intra- and intercellular VIGS to a greater extent than *TcvGFP* transcripts. In contrast, different profiles were observed for siRNA$_{TcvVGFP}$ and siRNA$_{16cGFP}$ corresponding to the two less-similar regions (Region 1: TcvGFP$_{237-306}$ and 16cGFP$_{300-369}$; Region 2: TcvGFP$_{345-540}$ and 16cGFP$_{408-603}$) (Fig. 4A-E; Fig. 5A-E). TcvGFP$_{237-306}$ and TcvGFP$_{345-540}$ siRNAs were of low abundance and generally of sense polarity in the control and all RNAi lines (Fig. 4A-E). However, higher levels of 16cGFP$_{300-369}$ and 16cGFP$_{408-603}$ siRNAs were observed, a significant amount of which was antisense. As with the other GFP siRNAs, the levels of 16cGFP$_{300-369}$ and 16cGFP$_{408-603}$ siRNAs were much higher in *GfpDCL4Ai* and lower in *GfpDCL2Ai*, compared to *Gfp*, *GfpDCL1i* and *GfpDCL3Bi* (Fig. 5A-E).

These results demonstrate that *DCL4* and *DCL2* antagonistically affected the accumulation of siRNAs associated with intercellular VIGS. The reduction of siRNA$_{TcvGFP}$ and siRNA$_{16cGFP}$ in *GfpDCL2Ai* or the massive accumulation of these siRNAs in *GfpDCL4Ai* is likely to be due to the respective loss or gain-of-function of DCL2-dependent production of primary or secondary siRNAs in these RNAi lines.

Potential DCL2-processed/dependent siRNA Signals for Intercellular VIGS

In *Nb*, the DCL2-processed siRNAs (Fig. 4C; Fig. 5C) and/or DCL2-dependent siRNAs (produced by *DCL2*-activated pathways; Fig. 4E; Fig. 5E) are likely to be involved in the intercellular spread of epidermal cell-originating VIGS. Consistent with this idea, an elevated level of 22nt siRNAs was only found in TCV/GFPΔCP-inoculated *GfpDCL4Ai* and *GfpDCL4Bi* plants that exhibited increased intercellular VIGS (Fig. 1; Supplemental

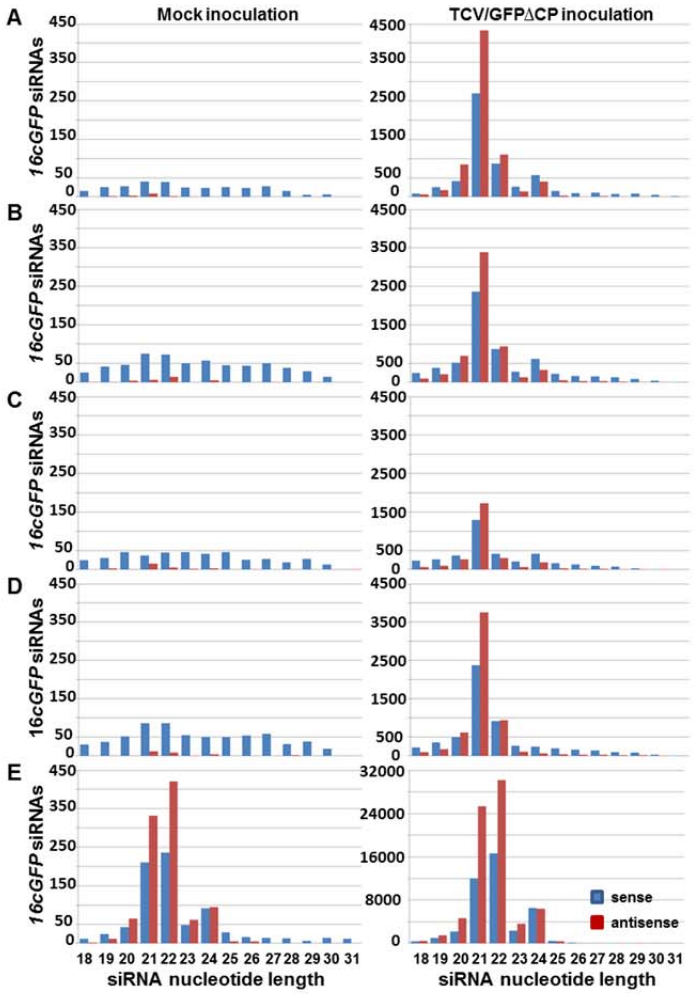

Figure 6. Size Profiles of Transgene *GFP* siRNA$_{16cGFP}$. (A) *Gfp*. (B) *GfpDCL1i*. (C) *GfpDCL2Ai*. (D) *GfpDCL3Bi*. (E) *GfpDCL4Ai*. The sRNA libraries were generated from sRNA samples extracted from leaves with mock (left) or TCV/GFPΔCP (right) inoculation. Blue and red bars represent siRNAs aligned to the sense and antisense strands of the transgene *16cGFP* mRNA respectively.

293 Fig. S9). To examine this correlation further, we analyzed the size profiles of sense and
294 antisense siRNA$_{16cGFP}$ (Fig. 6). The 21, 22 and 24nt siRNA$_{16cGFP}$ displayed similar size-
295 profiles between *Gfp* and *GfpDCL1i* (Fig. 6A and B, right panel). There was an obvious
296 reduction in 24nt siRNA$_{16cGFP}$ in *GfpDCL3Bi* (Fig. 6D, right panel). However among *Gfp*,

297 *GfpDCL1i* and *GfpDCL3Bi*, the 21nt siRNA$_{16cGFP}$ was always dominant while the levels
298 of 22nt siRNAs remained similar (Fig. 6A, B and D, right panel; Supplemental Table S4).
299 These findings further indicate that *DCL1*, *DCL3*, and DCL3-processed 24nt siRNAs
300 may not significantly contribute to cell-to-cell spread of VIGS, consistent with the results
301 of the local silencing assays (Fig. 1H-U).
302 RNAi of *DCL2* or *DCL4* imposed contrasting effects on the accumulation of 21,
303 22 and 24nt siRNA$_{16cGFP}$. Compared to *Gfp*, *GfpDCL1i* and *GfpDCL3Bi* (Fig. 6A, B and
304 D, right panel), the absolute reads of 21, 22 and 24nt siRNA$_{16cGFP}$ reduced in *GfpDCL2Ai*
305 (Fig. 6C, right panel), and markedly increased in *GfpDCL4Ai* (Fig. 6E, right panel).
306 Nonetheless, the percentage of the 22nt siRNA$_{16cGFP}$ decreased in *GfpDCL2Ai* whilst the
307 relative abundance of 21nt siRNA$_{16cGFP}$ reduced in *GfpDCL4Ai* (Supplemental Table S4).
308 These are in accordance with the respective roles of DCL4 and DCL2 in 21 and 22nt
309 siRNA biosynthesis. The levels of DCL2-processed 22nt siRNA$_{16cGFP}$ and DCL2-
310 dependent siRNA$_{16cGFP}$ were particularly low in *GfpDCL2Ai* (Fig. 6C, right panel), but
311 copious in *GfpDCL4Ai* (Fig. 5E, right panel; Supplemental Table S4), consistent with the
312 observed attenuation or enhancement of intercellular VIGS in the RNAi plants
313 respectively (Fig. 1). We also analyzed the size profiles of sense and antisense vsiRNA
314 (Fig. 7). Distributions of 18–31-nt vsiRNAs were not obviously altered among *Gfp*,
315 *GfpDCL1i*, *GfpDCL2Ai* and *GfpDCL3Bi* (Fig. 7A-D, right panel). In these RNAi lines,
316 the majority of vsiRNAs were 21nt in length (Fig. 7; Supplemental Table S4). However
317 in *GfpDCL4Ai*, vsiRNAs shifted their sizes largely to 22nt although there were also
318 marked increases in 21 and 24nt vsiRNAs (Fig. 7E, right panel). Notably, there was an
319 approximate 10% reduction of 22-nt vsiRNAs in *GfpDCL2Ai* compared to the *Gfp*
320 control (Supplemental Table S4). Taken together, our data show that *DCL4* plays a major,
321 and *DCL2* a minor, role in producing 21 or 22nt vsiRNAs for intracellular VIGS, whilst
322 *DCL2* is required to generate and perceive DCL2-processed/dependent mobile signals for
323 intercellular VIGS. These conclusions are further supported by similar results that were
324 generated from six extra sRNA libraries for the *Gfp* control and two different RNAi lines
325 *GfpDCL2Bi* and *GfpDCL4Bi* (Supplemental Fig. S10A-E).
326
327

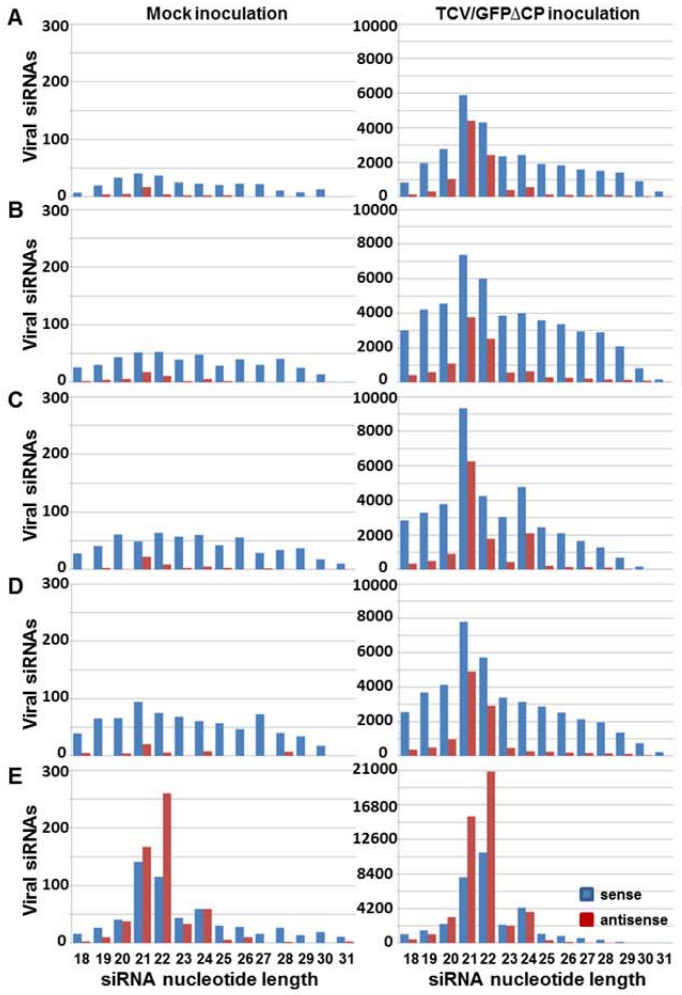

Figure 7. Size Profiles of TCV/GFPΔCP Viral siRNAs. (A) *Gfp*. (B) *GfpDCL1i*. (C) *GfpDCL2Ai*. (D) *GfpDCL3Bi*. (E) *GfpDCL4Ai*. The sRNA libraries were generated from sRNA samples extracted from leaves with mock (left) or TCV/GFPΔCP (right) inoculation. Blue and red bars represent siRNAs aligned to the sense and antisense strands of TCV/GFPΔCP RNA, respectively.

DISCUSSION

In plants, *DCLs* play diverse roles in sense- and hairpin RNA-mediated PTGS and TGS (Parent et al., 2015; Mlotshwa et al., 2008; Xie et al., 2004; 2005). *DCL4*, *DCL2* and their cognate 21 and 22nt vsiRNAs are involved in cell-autonomous VIGS but their antiviral

functioning roles are debated (Bouche et al., 2006; Fusaro et al, 2006; Garcia-Ruiz et al, 2010; Qu et al., 2008).

In this study, we reveal several interesting findings:

(1) RNAi of the four *DCL* genes does not affect cell-to-cell movement deficiency of the immobile virus TCV/GFPΔCP (Fig.1). This is consistent with our previous report that compromising of silencing machinery alone was not sufficient to promote virus movement (Shi et al., 2009). These findings ensure that any intercellular VIGS that we observe in our assays do not result from cell-to-cell movement of the recombinant viral RNA, and also argue against the idea that an altered ability to establish intra- and intercellular VIGS in these *DCL* DNAi lines may enable TCV-GFPΔCP to move locally or systemically more than in wild-type *Nb* plants.

(2) *DCL4* inhibited non-cell autonomous intercellular VIGS whilst it acted as a major trigger for intracellular VIGS (Fig. 3), consistent with its critical role in cell-autonomous silencing and vsiRNA biogenesis (Wang et al., 2011; Xie et al., 2005). Our findings are also in agreement with previous reports that *dcl4* mutations enhance transitivity of cell-autonomous PTGS and can rescue phloem-originating PTGS in *Arabidopsis* (Mlotshwa et al., 2008; Parent et al., 2015). The fact that *DCL4* attenuates intercellular VIGS implies that DCL4-processed 21nt vsiRNAs are unlikely to be involved in cell-to-cell spread of VIGS in *Nb*.

(3) *DCL2*, probably along with DCL2-processed/dependent siRNAs and their precursor RNAs, is involved in intercellular VIGS. *DCL2* was also able to target and degrade viral RNAs in plant cells but this activity was largely redundant when functional *DCL4* was present (Fig. 3). These findings suggest that *DCL2* could influence intracellular VIGS in *Nb* although *DCL2* is thought to be dispensable for antiviral silencing in *Arabidopsis* (Wang et al., 2011). Neither *DCL1* nor *DCL3* affected vsiRNA production or intra- and intercellular VIGS. Intriguingly, *DCL2* played a key role in spreading VIGS from individual epidermal cell to adjacent epidermal and mesophyll cells, a formerly unidentified function in silencing-based antiviral defense.

(4) Silencing machinery degraded *TcvGFP* mRNA and the resultant $siRNA_{TcvGFP}$ targeted identical regions in the transgene *16cGFP* mRNA and generated $siRNA_{16cGFP}$ for intracellular VIGS in TCV/GFPΔCP-infected epidermal cells (Figs. 4-7). Such

363 siRNA$_{TcvGFP}$ and siRNA$_{16cGFP}$ in sense and antisense polarities then led to biogenesis of
364 siRNAs associated with different parts across the *16cGFP* and *TcvGFP* RNA sequences
365 for intra- and intercellular VIGS. Our results thus imply that initial signals for
366 intercellular VIGS might consist of sense and antisense siRNA$_{TcvGFP}$ and siRNA$_{16cGFP}$.
367 Production of such signals in incipient epidermal cell (*i.e.* the TCV/GFPΔCP-infected
368 cell) and subsequent induction of *16cGFP* silencing in neighboring recipient cells (*i.e.*
369 TCV/GFPΔCP non-infected cells) were influenced positively by *DCL2*, but negatively by
370 *DCL4* (Fig. 1; Fig. 2). However, in contrast to complete loss-of-function genetic mutants,
371 RNAi lines are partial loss of function. It is also possible that TCV/GFPΔCP infection
372 could alter the expression of the *DCL* genes targeted by RNAi. Sequenced small RNAs
373 were from all of the cells in the inoculated leaves, including the inducing and recipient
374 cells. Considering these factors, it remains possible that long dsRNA precursors of DCL2
375 (or DCL4) could move between cells or long distance for induction of non-cell
376 autonomous VIGS.
377 Collectively, our results suggest that *DCL4* and *DCL2* play major but distinct
378 roles in intra-/intercellular VIGS. Involvement of *DCL2* and DCL2-processed/dependent
379 siRNAs as well as their precursor RNAs in intercellular VIGS is consistent with the fact
380 that DCL2 and DCL2-processed 22nt siRNA can effectively trigger biogenesis of
381 secondary siRNAs in plants (Chen et al., 2010), and restore intercellular PTGS induced
382 by sense- and hairpin-transgene RNAs in the *Arabidopsis dcl4* mutant (Mlotshwa et al.,
383 2008; Parent et al., 2015). It should be pointed out that silencing spread in our system is
384 more complex than other systems since it is dependent on the expression of both p8 and
385 p9 proteins of TCV (Zhou et al., 2008). Therefore, we are cautious to expand our findings
386 to other examples of cell-to-cell spread of RNA silencing, such as the controversial
387 *Arabidopsis* model in which, *DCL4* and DCL4-processed 21-nt siRNAs are thought to be
388 directly involved in short-range cell-to-cell spread of phloem-originating PTGS.
389 Nevertheless, our findings support a hypothesis that *DCL4* is essential for cell-
390 autonomous intracellular VIGS, but negatively regulates intercellular VIGS. This is likely
391 to be achieved via *DCL4*-mediated epistatic interference over *DCL2* because the latter is
392 essential to promote cell-to-cell spread of VIGS. Indeed *DCL4* can suppress the
393 expression of *DCL2* in *Nb* (Fig. 2). *DCL2* is also required to generate and perceive

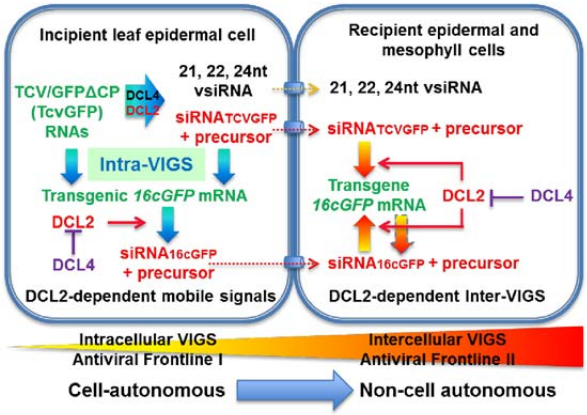

Figure 8. Cell- and Non-cell Autonomous VIGS in *N. benthamiana*. In incipient leaf epidermal cells (*i.e.* individual cells initially infected by TCV/GFPΔCP), *DCL4* plays a critical role in biogenesis of vsiRNAs, $siRNA_{TCVGFP}$ and transgene $siRNA_{16cGFP}$. These siRNAs are associated with cell-autonomous intracellular VIGS (Intra-VIGS) to inhibit local virus infection. DCL4-processed siRNAs are unlikely involved in spread of VIGS from leaf epidermal cell to adjacent cells because *DCL4* inhibits intercellular VIGS. In the incipient cell, *DCL2* can also target and dice viral RNAs, *TcvGFP* and *16cGFP* mRNA into siRNAs, but this activity is largely blocked by *DCL4* (**T** sign). In contrast, the key functionality of *DCL2* is to trigger efficient intercellular VIGS (Inter-VIGS). This is likely achieved through its activities to produce DCL2-processed/dependent siRNAs (and/or their precursor long RNAs, highlighted red) in incipient cells and to perceive these mobile signals for non-cell autonomous inter-VIGS in recipient epidermal and mesophyll cells. Neither *DCL1* nor *DCL3* affects vsiRNA production, intra- and intercellular VIGS. Thus *DCL4* and *DCL2* play major but distinct roles in cell- and non-cell autonomous VIGS that form a dual antiviral frontline in incipient and recipient cells. *DCL4*, the primary defender for the cell-autonomous intracellular VIGS, can attack viruses within the initially infected cells. However, if viruses break through this defence frontline, non-cell autonomous intracellular VIGS can efficiently spread to nearby recipient cells. This is due to loss of the negative control of intercellular VIGS mediated by *DCL4*. Intercellular VIGS is dependent upon functional *DCL2* and DCL2-processed/dependent siRNAs (and/or their precursor long RNAs), but it is negatively controlled by *DCL4*. RNAi of *DCL4* results in fully functional *DCL2* that enhances cell-to-cell spread of VIGS. The intercellular VIGS can then defend recipient cells from further virus infection. Such a dual-defence strategy can compensate each other to give host cells evolutionary advantage to battle against virus infection. This model is relevant to virus-VIGS interaction at the intra-/intercellular level, rather than to systemic virus infection. The potential spread of DCL2-processed/dependent siRNAs (and their precursor long RNAs, highlighted red) to move from the incipient to recipient cell through plasmodesmata is indicated with dashed arrows and cylinder signs.

394 mobile signals for systemic PTGS whilst *DCL4* inhibits systemic PTGS (Fan et al., 2017,
395 under revision). To put these findings in the context of RNA silencing-based defence, we
396 propose two separate components of an integrated viral defence strategy in which *DCL2*
397 and *DCL4* play different roles (Fig. 8). *DCL4*, the primary defender in the cell-

autonomous intracellular VIGS, attacks viruses within the initially infected cells. Simultaneously it also inhibits non-cell autonomous silencing. Thus, if this intracellular VIGS frontline in incipient cells was broken, for example through inhibiting *DCL4* activity by VSR such as P1/HC-Pro and P38 (Csorba et al., 2015; Mlotshwa et al, 2008), intercellular VIGS would then be activated efficiently spreading to nearby recipient cells to form a second frontline against the virus. Non-cell autonomous intercellular VIGS relies upon functional *DCL2* and DCL2-processed/dependent siRNAs and their precursor RNAs. In this scenario, *DCL2* is required to trigger the intercellular VIGS frontline and defend recipient cells from further virus invasion. *DCL2* may also contribute to cell-autonomous VIGS, but *DCL2* can only fulfil this activity when *DCL4* is absent or dysfunctional. This explains why an increased intercellular VIGS was observed in *DCL4* RNAi plants, but a deceased non-cell autonomous VIGS in *DCL2* RNAi plants. Such a local dual-defence strategy would be more difficult for the virus to breakdown and may provide plants with an evolutionary advantage in their defence against viral pathogens (Supplemental Text S3).

MATERIALS AND METHODS

Plant Materials and Growth Conditions

Wild-type *Nicotiana benthamiana* (*Nb*) and transgenic lines (Supplemental Table S1) were grown and maintained in insect-free growth-rooms at 25°C with supplementary lighting to give a 16-hour photoperiod.

Plasmid Constructs, Virus Inoculation and Microscopy

Construction of TCV/GFPΔCP was previously described (Ryabov et al., 2004). The full-length GFP sequence was PCR amplified using TCV/GFPΔCP as DNA template and cloned into pMD18-T (Takara) to produce pT7.GFP construct from which *GFP* RNA transcripts were produced by *in vitro* transcription using T7 RNA polymerase. Primers used for making this construct are listed in Supplemental Table S5. TCV/GFPΔCP RNA was generated by *in vitro* transcription and used to mechanically inoculate *Nb*, *DCL* RNAi, *16cGFP*, *Gfp*, *GfpDCL* RNAi plants as described (Ryabov et al., 2004).

Inoculated leaves were collected and visualized under a Zeiss Axiphot microscope as described (Ryabov et al., 2004).

Intra- and Intercellular VIGS Assays

We used a cell-specific, silencing suppression-free and movement-deficient Turnip crinkle virus (TCV/GFPΔCP)-based system to induce intracellular VIGS in a single epidermal cell, from which silencing spreads to form visible silencing foci covering 100-300 epidermal cells, equivalent to a circular area with a radius of 6-10 epidermal cells, on the leaf epidermis of transgenic *16cGFP* plants (Qin et al., 2012; Ryabov et al., 2004; Zhou et al., 2008). Of important notes, the precise location of a single epidermal cell that was initially infected with the movement-defective TCV/GFPΔCP could not be located prior to development of a visible silencing focus from the infected cell. Due to the compact TCV genome organization and viral gene expression strategy (Carrington et al., 1989; Cohen et al., 2000), it would be almost impossible to clone a second reporter gene, in addition to *GFP*, into TCV/GFPΔCP as an extra marker for measuring the initial infection of individual epidermal cell. Nevertheless, visible *GFP* silencing foci are a good indicator for induction and spread of TCV/GFPΔCP-induced intracellular VIGS. Upon mechanic inoculation, their appearance is a gradual process starting from the individual cell on the upper epidermises which is initially infected by TCV/GFPΔCP. Intracellular *GFP* silencing is induced by TCV/GFPΔCP in the single epidermal cell; and subsequently moves horizontally and vertically to neighboring upper epidermal, mesophyll and lower epidermal cells in a three-dimensional manner, i.e. occurrence of intercellular VIGS (Qin et al., 2012; Zhou et al., 2008).

To perform intra- and intercellular VIGS assays, a single young leaf (2nd from top) of each of four-to-six seedlings (six-leaf stage) of *16cGFP*, *Gfp GfpDCL1i*, *GfpDCL2Ai*, *GfpDCL2Bi*, *GfpDCL3Ai*, *GfpDCL3Bi*, *GfpDCL4Ai* or *GfpDCL4Bi* lines were mechanically inoculated with an equal amount of RNA transcripts produced by *in vitro* transcription from 2.5-μg *Pac*I-linearized TCV/GFPΔCP plasmid DNA as described (Ryabov et al., 2004). Induction and spread of *GFP* silencing was routinely examined under long-wavelength UV light and recorded photographically using a Nikon Digital Camera D7000. Regions of leaf lamina in which silencing of *GFP* mRNA occurred show

red chlorophyll fluorescence, while tissues expressing GFP show green fluorescence under long-wavelength UV light. Numbers and sizes of *GFP* silencing foci (dark patches) were counted, measured and photographed under a Zeiss Axiphot microscope using settings to visualize GFP green fluorescence as described (Qin et al., 2012). Number of silencing foci on an individual leaf was normalized against the average number of silencing foci per leaf of the control plants (i.e. *16cGFP* as control for *GfpDCL1i*, and *Gfp* as control for *GfpDCL2Ai*, *GfpDCL2Bi*, *GfpDCL3Ai*, *GfpbDCL3Bi*, *GfpDCL4Ai*, *GfpDCL4Bi* and *GfpDCL24i*) to minimize disparities that could be caused by experimental variations such as leaf sizes among different plants and freshly-generated inoculum RNA transcripts used in different experiments. SCI was calculated as percentage between the numbers of silencing foci counted on lower and upper (inoculated side) epidermises. Intra- and intercellular VIGS assays were performed for each of the transgenic lines in at least two separate experiments.

RNA Extraction and Northern Hybridization

For quantitative Real-Time PCR (qRT-PCR), total RNAs were extracted from leaf tissues using the RNAprep Pure Plant Kit (Tiangen) as recommended by the manufacturer. For Northern blot, total RNAs were extracted from leaf tissues with Trizol reagent (Invitrogen, Carlsbad, CA) as recommended by the manufacturer. To analyze siRNAs, low-molecular-mass small RNAs were enriched from total RNA as previously described (Hamilton and Baulcombe, 1999). The enriched small RNAs (2.5μg) were fractionated on an 18% denaturing polyacrylamide–7 M urea gel in 1 x Tris–borate–EDTA (TBE) buffer. Small RNAs were transferred to Hybond-N+ membranes (Amersham Biosciences) by upward capillary transfer in 20xSSC buffer, then cross-linked to the membranes with an UVP CX 2000 UV Crosslinker for 4 times (upside, underside, upside, underside) at 120 millijoules/cm^2, 1 minute each time. The membranes were hybridized with digoxigenin (Dig)-labelled *GFP* RNA probes prepared by in vitro transcription using pT7.GFP and DIG RNA Labeling Kit (Roche) as recommended by the manufacturer. The hybridization chemiluminescence signals were detected with a ChemiDoc^{TM} XRS+ imaging System (Bio Rad).

qRT-PCR

TCV/GFPΔCP or mock-inoculated leaves of *Nb*, *DCL* RNAi, *16cGFP, Gfp*, and *GfpDCL* RNAi plants were taken at 7 days post inoculation in three repeated experiments for RNA extraction. The first-stranded cDNA was synthesized using total RNAs treated with RNase-free DNase I as templates by the M-MLV Reverse Transcriptase (Promega). The qRT–PCR analyses of *DCLs* mRNA or TCV/GFPΔCP RNA levels were performed using specific primers (Supplemental Table S5) and the SYBR Green Mix, The amplification program for SYBR Green I was performed at 95ºC for 10 seconds, 58ºC for 30 seconds and 72ºC for 20 seconds on the CFX96 machine (Bio-Rad), following the manufacturer's instructions. Quadruplicate quantitative assays (four technical replicates) were performed on cDNA of each of three-four biological duplicates (leaf tissues from three-four different treated plants). The relative RNA quantification was calculated using the formula $2^{-\Delta\Delta Ct}$ and normalized to the amount of GAPDH (Genbank accession number TC17509) as described (Qin et al., 2012).

Construction of sRNA Library and sRNA Sequencing

Fragments of 18-30 bases long RNA were isolated from total RNA extracted from mock- or TCV/GFPΔCP-inoculated leaf tissues of 3-4 different plants collected at seven days post-inoculation (dpi) after being separated through 15% denaturing PAGE. Then sRNAs were excised from the gel and sequentially ligated to 3'- and 5'-adapters. After each ligation step, sRNAs were purified after 15% denaturing PAGE. The final purified ligation products were reversely transcribed into cDNA using reverse transcriptase (Finnzymes Oy). The first strand cDNA was PCR amplified using Phusion* DNA Polymerase (Finnzymes Oy). The purified DNA fragments were used for clustering and sequencing by Illumina Hiseq 2000 (Illumina, San Diego, CA) at the Beijing Genomics Institute, Shenzhen. It should be noted that a pool of leaves from 3-4 different plants was used for construction of each sRNA library. This avoided potential variations between individual treated plants, in particular these for TCV/GFPΔCP-based intra- and intercellular VIGS assays due to some variations of TCV/GFPΔCP replication in different plants.

Bioinformatics Analysis of sRNA Sequences

Illumina HighSeq 2000 sequencing produced 11 to 12 million reads per sRNA library. The reads were cropped to remove adapter sequences and were aligned to the reference sequences using Bowtie2 (Langmead and Salzberg, 2012; Ryabov et al., 2014). The reference sequences included TCV/GFPΔCP, viral *TcvGFP* and *16cGFP* transgene (Haseloff et al., 1997; Ruiz et al., 1998; Ryabov et al., 2004), *DCL1*, *DCL2*, *DCL3* and *DCL4* gene sequences (Nakasugi et al., 2013) and the set of 50 tobacco microRNAs identified in *Nicotiana* plants (Nakasugi et al., 2014; Pandey et al., 2008). SAMtools pileup was used to produce the siRNA and miRNA coverage profiles. For correlation analyses for the six small RNA libraries, we determined numbers of the miRNA hits corresponding to the previously identified set of 50 *Nicotiana* miRNAs (Nakasugi et al., 2014; Pandey et al., 2008). All analyzed small RNA libraries contained similar proportions of host-encoded miRNA reads (Supplemental Dataset S1; Supplemental Dataset S2; Supplemental Dataset S3), indicating equivalence and direct comparability of the sRNA datasets. Indeed outcomes of comparisons between normalized siRNAs generated from target sequences against the total sRNA reads for all the libraries (per 10 million sRNA reads) are consistent with that the reads of siRNAs were directly compared.

Statistical Analysis

Normalized number of RNA silencing foci per leaf, sizes of RNA silencing foci, "silencing cell-to-cell-spread index" (SCI) and qRT-PCR data between control and various treatments were analysed by Student's ***t***-Tests using an online programme (http://www.physics.csbsju.edu/stats/t-test.html). It is worthwhile noting that approximately 4% or more change in the silencing foci sizes is of statistical significance due to the large numbers of samples (80-560) tested between wild-type controls and RNAi lines (Fig. 1; Supplemental Table S2).

Supplemental Data

The following materials are available in the online version of this article.

Supplemental Text S1. Parameters for Assessing Intra- and Intercellular VIGS.

552 **Supplemental Text S2.** *DCLs* Play Differential Roles in vsiRNA Biogenesis**.**

553 **Supplemental Text S3.** Local VIGS vs Virus Interaction at the Intra-/intercellular Level.

554 **Supplemental Figure S1.** Total small RNA Profiles.

555 **Supplemental Figure S2.** Distribution of vsiRNAs and $siRNA_{TcvGFP}$ across the
556 TCV/GFPΔCP RNA.

557 **Supplemental Figure S3.** Distribution of vsiRNAs across the TCVΔCP RNA.

558 **Supplemental Figure S4.** Distribution of vsiRNAs across the TCVΔCP RNA.

559 **Supplemental Figure S5.** Impact of *NbDCLi* on TCV/GFPΔCP RNA Replication.

560 **Supplemental Figure S6.** Comparisons between Transgene *16cGFP* and Viral *TcvGFP*
561 Sequences.

562 **Supplemental Figure S7.** Distribution of 20-25nt *GFP* siRNAs Across the 714nt
563 *TcvGFP* mRNA.

564 **Supplemental Figure S8.** Distribution of 20-25nt *GFP* siRNAs Across the 792nt
565 Transgene *16cGFP* mRNA.

566 **Supplemental Figure S9.** Northern Detection of TCV/GFPΔCP siRNAs.

567 **Supplemental Figure S10.** *NbDCL2* and NbDCL2-dependent siRNAs for Non-cell
568 Autonomous Intercellular VIGS.

569 **Supplemental Table S1.** *NbDCL* RNAi Lines Used in This Study.

570 **Supplemental Table S2.** Impact of *DCL* RNAi on Cell-to-cell Spread of Virus-induced
571 RNA Silencing.

572 **Supplemental Table S3.** Percentage of *16cGFP* and TCV/GFPΔCP 21-, 22- and 24-nt
573 siRNA.

574 **Supplemental Table S4**. Summary of Total Viral and/or GFP siRNAs in Mock- or
575 TCV/GFPΔCP-inoculated Leaves.

576 **Supplemental Table S5.** Primers Used in This Study.

577 **Supplemental Dataset S1.** Summary of sRNA and miRNA reads.

578 **Supplemental Dataset S2**. Correlation analyses of miRNA profiles among 10 sRNA
579 libraries.

580 **Supplemental Dataset S3.** Comparisons of miRNAs among ten sRNA libraries.

581

582 ## ACKNOWLEDGEMENTS

We are grateful to David Baulcombe for his kind gift of the transgenic line *16cGFP* and *RDR6i* seeds. The corresponding author thanks Dr Alison Tör for checking English grammar and style throughout the manuscript.

FIGURE LEGENDS

Figure 1. Different Roles of *DCLs* in the Cell-to-cell Spread of VIGS. (A) Down-regulation of *DCL* expression by RNAi. Young leaves were collected from *DCL* RNAi plants at 7 days post-inoculation (dpi), and the level of *DCL* RNAs was analysed by qRT-PCR. (B) Schematic of the intracellular RNA silencing trigger TCV/GFPΔCP. The T7 promoter, viral RNA-dependent RNA polymerases (P28, P88), movement proteins (P8 and P9) and GFP are indicated. (C-G) Restricted localization of TCV/GFPΔCP in single epidermal cell of *Nb* (C), *DCL1i* (D) *DCL2Ai* (E), *DCL3Bi* (F) and *DCL4Ai* (G) plants. (H-Q) Intercellular *GFP* silencing foci (dark patches indicated by red arrows). Photographs of silencing foci on leaves of *16cGFP* (H); *GfpDCL1i* (I); *Gfp* (J); *GfpDCL2Ai* (K) and *GfpDCL2Bi* (L); *GFPDCL3Ai* (M) and *GfpDCL3Bi* (N); *GfpDCL4Ai* (O) and *GfpDCL4Bi* (P); and a triple-cross line *GfpDCL24i* (Q), were taken under a fluorescent microscope at 7 dpi. Bar=500μm. (R) Normalized number of *GFP* silencing foci per upper epidermis. Silencing foci were counted at 7 dpi from 3-21 different plant leaves inoculated with TCV/GFPΔCP. (S) and (T) Average size (diameters, S) and percentage change (T) of silencing foci. 80-560 silencing foci on different upper epidermises were randomly selected and measured. (U) SCI calculated as percentage of number of silencing foci on lower epidermis out of the number of silencing foci on upper epidermis. Student's ***t***-tests were performed for qRT-PCR and silencing data (mean ± standard deviation) and P-values are indicated (asterisks).

Figure 2. Regulation of *DCL2* Expression by *DCL3* and *DCL4*. (A-C) Effects of RNAi of *DCL2* (A), *DCL3* (B) and *DCL4* (C) on *DCL* gene expression. Young leaf tissues were collected at 6-8 leaf stage from four different plants of each transgenic line as indicated. RNA transcripts were analysed by qRT-PCR. Four technical replicates for qRT-PCR assays were performed on each cDNA of four biological duplicates (n = 4; leaf tissues from four different transgenic plants). Student's ***t***-tests were performed for data (mean ±

614 standard deviation) and P-values are indicated (asterisks). *DCL2i* does not affect
615 expression of *DCL1*, *DCL3* or *DCL4* (A). However *DCL3i* (B) or *DCL4i* (C) resulted in
616 increased mRNA levels of *DCL2*.
617
618 **Figure 3. Distribution of 20-25nt vsiRNAs and siRNA$_{TcvGFP}$ across the**
619 **TCV/GFPΔCP RNA.** (A) *Gfp*. (B) *GfpDCL1i*. (C) *GfpDCL2Ai*. (D) *GfpDCL3Bi*. (E)
620 *GfpDCL4Ai*. The sRNA libraries were generated from sRNA samples extracted from
621 TCV/GFPΔCP-inoculated leaves. Blue and red bars represent siRNAs aligned to the
622 sense (positive) and antisense (negative) strands of TCV/GFPΔCP viral RNA and
623 *TcvGFP* mRNA (highlighted), respectively. The TCV/GFPΔCP genome organisation is
624 indicated.
625
626 **Figure 4. Distribution of 20-25nt *GFP* siRNAs across the 714nt *TcvGFP* mRNA.** (A)
627 *Gfp*. (B) *GfpDCL1i*. (C) *GfpDCL2Ai*. (D) *GfpDCL3Bi*. (E) *GfpDCL4Ai*. The sRNA
628 libraries were generated from sRNA samples extracted from TCV/GFPΔCP-inoculated
629 leaves. Blue and red bars represent siRNAs aligned to the sense (positive) and antisense
630 (negative) strands of *TcvGFP* mRNA, respectively. The two regions (Region 1 and
631 Region 2) having less sequence similarity with that of the transgene *16cGFP* mRNA (see
632 Fig. 5) as well as nucleotide coordinates are indicated.
633
634 **Figure 5. Distribution of 20-25nt *GFP* siRNAs across the 792nt Transgene *16cGFP***
635 **mRNA.** (A) *Gfp*. (B) *GfpDCL1i*. (C) *GfpDCL2Ai*. (D) *GfpDCL3Bi*. (E) *GfpDCL4Ai*. The
636 sRNA libraries were generated from sRNA samples extracted from TCV/GFPΔCP-
637 inoculated leaves. Blue and red bars represent siRNAs aligned to the sense (positive) and
638 antisense (negative) strands of *16cGFP* mRNA, respectively. The two regions (Region 1
639 and Region 2) having less sequence similarity with that of the transgene *TcvGFP* mRNA
640 (see Fig. 4) as well as nucleotide coordinates are indicated.
641
642 **Figure 6. Size Profiles of Transgene *GFP* siRNA$_{16cGFP}$.** (A) *Gfp*. (B) *GfpDCL1i*. (C)
643 *GfpDCL2Ai*. (D) *GfpDCL3Bi*. (E) *GfpDCL4Ai*. The sRNA libraries were generated from
644 sRNA samples extracted from leaves with mock (left) or TCV/GFPΔCP (right)

inoculation. Blue and red bars represent siRNAs aligned to the sense and antisense strands of the transgene *16cGFP* mRNA respectively.

Figure 7. Size Profiles of TCV/GFPΔCP Viral siRNAs. (A) *Gfp*. (B) *GfpDCL1i*. (C) *GfpDCL2Ai*. (D) *GfpDCL3Bi*. (E) *GfpDCL4Ai*. The sRNA libraries were generated from sRNA samples extracted from leaves with mock (left) or TCV/GFPΔCP (right) inoculation. Blue and red bars represent siRNAs aligned to the sense and antisense strands of TCV/GFPΔCP RNA, respectively.

Figure 8. Cell- and Non-cell Autonomous VIGS in *N. benthamiana*. In incipient leaf epidermal cells (*i.e.* individual cells initially infected by TCV/GFPΔCP), *DCL4* plays a critical role in biogenesis of vsiRNAs, $siRNA_{TCVGFP}$ and transgene $siRNA_{16cGFP}$. These siRNAs are associated with cell-autonomous intracellular VIGS (Intra-VIGS) to inhibit local virus infection. DCL4-processed siRNAs are unlikely involved in spread of VIGS from leaf epidermal cell to adjacent cells because *DCL4* inhibits intercellular VIGS. In the incipient cell, *DCL2* can also target and dice viral RNAs, *TcvGFP* and *16cGFP* mRNA into siRNAs, but this activity is largely blocked by *DCL4* (**T** sign). In contrast, the key functionality of *DCL2* is to trigger efficient intercellular VIGS (Inter-VIGS). This is likely achieved through its activities to produce DCL2-processed/dependent siRNAs (and/or their precursor long RNAs, highlighted red) in incipient cells and to perceive these mobile signals for non-cell autonomous inter-VIGS in recipient epidermal and mesophyll cells. Neither *DCL1* nor *DCL3* affects vsiRNA production, intra- and intercellular VIGS. Thus *DCL4* and *DCL2* play major but distinct roles in cell- and non-cell autonomous VIGS that form a dual antiviral frontline in incipient and recipient cells. *DCL4*, the primary defender for the cell-autonomous intracellular VIGS, can attack viruses within the initially infected cells. However, if viruses break through this defence frontline, non-cell autonomous intracellular VIGS can efficiently spread to nearby recipient cells. This is due to loss of the negative control of intercellular VIGS mediated by *DCL4*. Intercellular VIGS is dependent upon functional *DCL2* and DCL2-processed/dependent siRNAs (and/or their precursor long RNAs), but it is negatively controlled by *DCL4*. RNAi of *DCL4* results in fully functional *DCL2* that enhances cell-

676 to-cell spread of VIGS. The intercellular VIGS can then defend recipient cells from
677 further virus infection. Such a dual-defence strategy can compensate each other to give
678 host cells evolutionary advantage to battle against virus infection. This model is relevant
679 to virus-VIGS interaction at the intra-/intercellular level, rather than to systemic virus
680 infection. The potential spread of DCL2-processed/dependent siRNAs (and their
681 precursor long RNAs, highlighted red) to move from the incipient to recipient cell
682 through plasmodesmata is indicated with dashed arrows and cylinder signs.
683
684

Parsed Citations

Aliyari, R. and Ding, S.W. (2009). RNA-based viral immunity initiated by the Dicer family of host immune receptors. Immunol. Rev. 227: 176-188.
Pubmed: Author and Title
CrossRef: Author and Title
Google Scholar: Author Only Title Only Author and Title

Andika, I.B., Maruyama, K., Sun, L., Kondo, H., Tamada, T., and Suzuki, N. (2015). Differential contributions of plant Dicer-like proteins to antiviral defences against potato virus X in leaves and roots. Plant J. 81: 781-793.
Pubmed: Author and Title
CrossRef: Author and Title
Google Scholar: Author Only Title Only Author and Title

Aregger, M., Borah, B.K., Seguin, J., Rajeswaran, R., Gubaeva, E.G., Zvereva, A.S., Windels, D., Vazquez, F., Blevins, T., Farinelli, L., et al., (2012). Primary and secondary siRNAs in geminivirus-induced gene silencing. PLoS Pathog. 8: e1002941.
Pubmed: Author and Title
CrossRef: Author and Title
Google Scholar: Author Only Title Only Author and Title

Baulcombe, D. (2004). RNA silencing in plants. Nature 431: 356-363.
Pubmed: Author and Title
CrossRef: Author and Title
Google Scholar: Author Only Title Only Author and Title

Berg, J.M. (2016) Retraction. Science 354: 190.
Pubmed: Author and Title
CrossRef: Author and Title
Google Scholar: Author Only Title Only Author and Title

Blevins, T., Rajeswaran, R., Shivaprasad, P.V., Beknazariants, D., Si-Ammour, A., Park, H.S., Vazquez, F., Robertson, D., Meins, F. Jr., Hohn, T., et al. (2006). Four plant Dicers mediate viral small RNA biogenesis and DNA virus induced silencing. Nucleic Acids Res. 34: 6233-6246.
Pubmed: Author and Title
CrossRef: Author and Title
Google Scholar: Author Only Title Only Author and Title

Bouche, N., Lauressergues, D., Gasciolli, V., and Vaucheret, H. (2006).An antagonistic function for Arabidopsis DCL2 in development and a new function for DCL4 in generating viral siRNAs. EMBO J. 25: 3347-3356.
Pubmed: Author and Title
CrossRef: Author and Title
Google Scholar: Author Only Title Only Author and Title

Carrington, J.C., Heaton, L.A., Zuidema, D., Hillman, B.I., and Morris, T.J. (1989). The genome structure of turnip crinkle virus. Virology 170: 219-26.
Pubmed: Author and Title
CrossRef: Author and Title
Google Scholar: Author Only Title Only Author and Title

Chattopadhyay, M., Stupina, V.A., Gao, F., Szarko, C.R., Kuhlmann, M.M., Yuan, X., Shi, K., and Simon, A.E. (2015). Requirement for host RNA-silencing components and the virus-silencing suppressor when second-site mutations compensate for structural defects in the 3' untranslated region. J. Virol. 89: 11603-11618.
Pubmed: Author and Title
CrossRef: Author and Title
Google Scholar: Author Only Title Only Author and Title

Chen, H.M., Chen, L.T., Patel, K., Li, Y.H., Baulcombe, D.C., and Wu, S.H. (2010).22-nucleotide RNAs trigger secondary siRNA biogenesis in plants. Proc. Natl. Acad. Sci. USA 107: 15269-15274 (2010).
Pubmed: Author and Title
CrossRef: Author and Title
Google Scholar: Author Only Title Only Author and Title

Cohen, Y., Gisel, A., and Zambryski, P.C. (2000). Cell-to-cell and systemic movement of recombinant green fluorescent protein-tagged turnip crinkle viruses. Virology 273: 258-266
Pubmed: Author and Title
CrossRef: Author and Title
Google Scholar: Author Only Title Only Author and Title

Csorba, T., Kontra, L., and Burgyan, J. (2015). Viral silencing suppressors: Tools forged to fine-tune host-pathogen coexistence. Virology 479-480: 85-103.
Pubmed: Author and Title
CrossRef: Author and Title
Google Scholar: Author Only Title Only Author and Title

Dunoyer, P., Himber, C., and Voinnet, O. (2005). DICER-LIKE 4 is required for RNA interference and produces the 21-nucleotide small interfering RNA component of the plant cell-to-cell silencing signal. Nat. Genet. 37: 1356-1360.
Pubmed: Author and Title
CrossRef: Author and Title
Google Scholar: Author Only Title Only Author and Title

Fusaro, A.F., Matthew, L., Smith, N.A., Curtin, S.J., Dedic-Hagan, J., Ellacott, G.A., Watson, J.M, Wang, M.B., Brosnan, C., Carroll, B.J., et al. (2006). RNA interference-inducing hairpin RNAs in plants act through the viral defence pathway. EMBO Rep. 7: 1168-1175.
Pubmed: Author and Title
CrossRef: Author and Title
Google Scholar: Author Only Title Only Author and Title

Garcia-Ruiz, H., Takeda, A., Chapman, E.J., Sullivan, C.M., Fahlgren. N., Brempelis, K.J., and Carrington, J.C. (2010). Arabidopsis RNA-dependent RNA polymerases and Dicer-like proteins in antiviral defense and small interfering RNA biogenesis during Turnip mosaic virus infection. Plant Cell 22: 481-496.
Pubmed: Author and Title
CrossRef: Author and Title
Google Scholar: Author Only Title Only Author and Title

Hacker, D.L., Petty, I.T., Wei, N., and Morris, T.J. (1992). Turnip crinkle virus genes required for RNA replication and virus movement. Virology 186: 1-8.
Pubmed: Author and Title
CrossRef: Author and Title
Google Scholar: Author Only Title Only Author and Title

Hamilton, A.J., and Baulcombe, D.C. (1999).A species of small antisense RNA in posttranscriptional gene silencing in plants. Science 286: 950-952.
Pubmed: Author and Title
CrossRef: Author and Title
Google Scholar: Author Only Title Only Author and Title

Haseloff, J., Siemering, K.R., Prasher, D.C., and Hodge, S. (1997). Removal of a cryptic intron and subcellular localization of green fluorescent protein are required to mark transgenic Arabidopsis plants brightly. Proc. Natl. Acad. Sci. USA 94: 2122-2127.
Pubmed: Author and Title
CrossRef: Author and Title
Google Scholar: Author Only Title Only Author and Title

Henderson, I.R., Zhang, X., Lu, C., Johnson, L., Meyers, B.C., Green, P.J., and Jacobsen, S.E. (2006). Dissecting Arabidopsis thaliana DICER function in small RNA processing, gene silencing and DNA methylation patterning. Nat. Genet. 38: 721-725.
Pubmed: Author and Title
CrossRef: Author and Title
Google Scholar: Author Only Title Only Author and Title

Langmead, B., and Salzberg, S. (2012). Fast gapped-read alignment with Bowtie 2. Nat. Methods 9: 357-359.
Pubmed: Author and Title
CrossRef: Author and Title
Google Scholar: Author Only Title Only Author and Title

Katsarou, K., Mavrothalassiti, E., Dermauw, W., Van Leeuwen, T., and Kalantidis, K. (2016) Combined Activity of DCL2 and DCL3 Is Crucial in the Defense against Potato Spindle Tuber Viroid. PLoS Pathog. 12: e1005936.
Pubmed: Author and Title
CrossRef: Author and Title
Google Scholar: Author Only Title Only Author and Title

Li, C., Zhang, K., Zeng, X., Jackson, S., Zhou, Y., and Hong, Y. (2009). A cis element within flowering locus T mRNA determines its mobility and facilitates trafficking of heterologous viral RNA. J. Virol. 83: 3540-3548.
Pubmed: Author and Title
CrossRef: Author and Title
Google Scholar: Author Only Title Only Author and Title

Li, W. Z., Qu, F., and Morris, T. J. (1998). Cell-to-cell movement of turnip crinkle virus is controlled by two small open reading frames that function in trans. Virology 244: 405-416.
Pubmed: Author and Title
CrossRef: Author and Title
Google Scholar: Author Only Title Only Author and Title

Melnyk, C.W., Molnar, A., and Baulcombe, D.C. (2011). Intercellular and systemic movement of RNA silencing. EMBO J. 30: 3553-3563.
Pubmed: Author and Title
CrossRef: Author and Title
Google Scholar: Author Only Title Only Author and Title

Merai, Z., Kerenyi, Z., Kertesz, S., Magna, M., Lakatos, L., and Silhavy, D. (2006). Double-stranded RNA binding may be a general plant RNA viral strategy to suppress RNA silencing. J. Virol. 80: 5747-5756.
Pubmed: Author and Title
CrossRef: Author and Title
Google Scholar: Author Only Title Only Author and Title

Mlotshwa, S., Pruss, G.J., Peragine, A., Endres, M.W., Li, J., Chen, X., Poethig, R.S., Bowman, L.H., and Vance, V. (2008). DICER-LIKE2 plays a primary role in transitive silencing of transgenes in Arabidopsis. PLoS One 3: e1755.
Pubmed: Author and Title
CrossRef: Author and Title
Google Scholar: Author Only Title Only Author and Title

Mukherjee, K., Campos, H., and Kolaczkowski, B. (2013). Evolution of animal and plant dicers: early parallel duplications and

recurrent adaptation of antiviral RNA binding in plants. Mol. Biol. Evol. 30: 627-641.
Pubmed: Author and Title
CrossRef: Author and Title
Google Scholar: Author Only Title Only Author and Title

Nakasugi, K., Crowhurst, R., Bally, J., and Waterhouse, P. (2014). Combining transcriptome assembly from multiple De novo assemblers in the allo-tetraploid plant Nicotiana benthamiana. PLoS One 9: e91776.
Pubmed: Author and Title
CrossRef: Author and Title
Google Scholar: Author Only Title Only Author and Title

Nakasugi, K., Crowhurst, R.N., Bally, J., Wood, C.C., Hellens, R.P., and Waterhouse, P.M. (2013). De novo transcriptome sequence assembly and analysis of RNA silencing genes of Nicotiana benthamiana. PLoS One 8: e59534.
Pubmed: Author and Title
CrossRef: Author and Title
Google Scholar: Author Only Title Only Author and Title

Pandey, S.P., Shahi, P., Gase, K., and Baldwin, I.T. (2008). Herbivory-induced changes in the small-RNA transcriptome and phytohormone signaling in Nicotiana attenuate. Proc. Natl. Acad. Sci. USA 105: 4559-4564.
Pubmed: Author and Title
CrossRef: Author and Title
Google Scholar: Author Only Title Only Author and Title

Parent, J-S., Bouteiller, N., Elmayan, T., and Vaucheret, H. (2015). Respective contribution of Arabidopsis DCL2 and DCL4 to RNA silencing. Plant J. 81: 223-232.
Pubmed: Author and Title
CrossRef: Author and Title
Google Scholar: Author Only Title Only Author and Title

Perez-Canamas, M., and Hernandez, C. (2015). Key importance of small RNA binding for the activity of a glycine-tryptophan (GW) motif-containing viral suppressor of RNA silencing. J. Biol. Chem. 290: 3106-3120.
Pubmed: Author and Title
CrossRef: Author and Title
Google Scholar: Author Only Title Only Author and Title

Qin, C., Shi, N., Gu, M., Zhang, H., Li, B., Shen, J., Mohammed, A., Ryabov, E., Li, C., Wang, H., et al. (2012). Involvement of RDR6 in short-range intercellular RNA silencing in Nicotiana benthimiana. Sci. Rep. 2: 467.
Pubmed: Author and Title
CrossRef: Author and Title
Google Scholar: Author Only Title Only Author and Title

Qu, F., Ren, T., and Morris, T. J. (2003).The coat protein of turnip crinkle virus suppresses posttranscriptional gene silencing at an early initiation step. J. Virol. 77: 511-522.
Pubmed: Author and Title
CrossRef: Author and Title
Google Scholar: Author Only Title Only Author and Title

Qu, F., Ye, X., and Morris, T.J. (2008). Arabidopsis DRB4, AGO1, AGO7, and RDR6 participate in a DCL4-initiated antiviral RNA silencing pathway negatively regulated by DCL1. Proc. Natl. Acad. Sci. USA 105: 14732-14737.
Pubmed: Author and Title
CrossRef: Author and Title
Google Scholar: Author Only Title Only Author and Title

Qu, J., Ye, J., and Fang, R. (2007). Artificial microRNA-mediated virus resistance in plants. J. Virol. 81: 6690-6699.
Pubmed: Author and Title
CrossRef: Author and Title
Google Scholar: Author Only Title Only Author and Title

Ryabov, E.V., van Wezel. R., Walsh, J., and Hong, Y. (2004). Cell-to-Cell, but not long-distance, spread of RNA silencing that is induced in individual epidermal cells. J. Virol. 78: 3149-3154.
Pubmed: Author and Title
CrossRef: Author and Title
Google Scholar: Author Only Title Only Author and Title

Ryabov, E.V., Wood, G.R., Fannon, J.M., Moore, J.D., Bull, J.C., Chandler, D., Mead, A., Burroughs, N., and Evans D.J. (2014). A virulent strain of Deformed Wing Virus (DWV) of Honeybees (Apis mellifera) prevails after Varroa destructor-mediated, or in vitro, transmission. PLoS Pathog. 10: e1004230.
Pubmed: Author and Title
CrossRef: Author and Title
Google Scholar: Author Only Title Only Author and Title

Ruiz, M.T., Voinnet, O., and Baulcombe, D.C. (1998). Initiation and maintenance of virus-induced gene silencing. Plant Cell 10: 937-946.
Pubmed: Author and Title
CrossRef: Author and Title
Google Scholar: Author Only Title Only Author and Title

Sarkies, P., and Miska, E.A. (2014). Small RNAs break out: the molecular cell biology of mobile small RNAs. Nat. Rev. Mol. Cell Biol. 15: 525-535.
Pubmed: Author and Title

CrossRef: Author and Title
Google Scholar: Author Only Title Only Author and Title

Schwach, F., Vaistij, F.E., Jones, L., and Baulcombe, D.C. (2005). An RNA-dependent RNA polymerase prevents meristem invasion by potato virus X and is required for the activity but not the production of a systemic silencing signal. Plant Physiol. 138: 1842-1852.
Pubmed: Author and Title
CrossRef: Author and Title
Google Scholar: Author Only Title Only Author and Title

Searle, I.R., Pontes, O., Melnyk, C.W., Smith, L.M., and Baulcombe, D.C. (2010). JMJ14, a JmjC domain protein, is required for RNA silencing and cell-to-cell movement of an RNA silencing signal in Arabidopsis. Genes Dev. 24: 986-991.
Pubmed: Author and Title
CrossRef: Author and Title
Google Scholar: Author Only Title Only Author and Title

Shi, Y., Ryabov, E.V., van Wezel, R., Li, C., Jin, M., Wang, W., Fan, Z., and Hong, Y. (2009). Suppression of local RNA silencing is not sufficient to promote cell-to-cell movement of Turnip crinkle virus in Nicotiana benthamiana. Plant Signal Behav. 4: 15-22.
Pubmed: Author and Title
CrossRef: Author and Title
Google Scholar: Author Only Title Only Author and Title

Smith, L.M., Pontes, O., Searle, I., Yelina, N., Yousafzai, F.K., Herr, A.J., Pikaard, C.S., and Baulcombe, D.C. (2007). An SNF2 protein assoicated with nuclear RNA silencing and the spread of a silencing signal between cells in Arabidopsis. Plant Cell 19: 1507-1521.
Pubmed: Author and Title
CrossRef: Author and Title
Google Scholar: Author Only Title Only Author and Title

Thomas, C.L., Leh, V., Lederer, C., and Maule, A.J. (2003). Turnip crinkle virus coat protein mediates suppression of RNA silencing in Nicotiana benthamiana. Virology 306: 33-41.
Pubmed: Author and Title
CrossRef: Author and Title
Google Scholar: Author Only Title Only Author and Title

Wang, X.B., Jovel, J., Udomporn, P., Wang, Y., Wu, Q., Li, W.X., Gasciolli, V., Vaucheret, H., and Ding, S.W. (2011).The 21-nucleotide, but not 22-nucleotide, viral secondary small interfering RNAs direct potent antiviral defence by two cooperative argonautes in Arabidopsis thaliana. Plant Cell 23: 1625-1638.
Pubmed: Author and Title
CrossRef: Author and Title
Google Scholar: Author Only Title Only Author and Title

Xie, Z., Allen, E., Wilken, A., and Carrington, J.C. (2005). DICER-LIKE 4 functions in trans-acting small interfering RNA biogenesis and vegetative phase change in Arabidopsis thaliana. Proc. Natl. Acad. Sci. USA 102: 12984-12989.
Pubmed: Author and Title
CrossRef: Author and Title
Google Scholar: Author Only Title Only Author and Title

Xie, Z., Johansen, L.K., Gustafson, A.M., Kasschau, K.D., Lellis, A.D., Zilberman, D., Jacobsen, S.E., and Carrington, J.C. (2004). Genetic and functional diversification of small RNA pathways in plants. PLoS Biol. 2: E104.
Pubmed: Author and Title
CrossRef: Author and Title
Google Scholar: Author Only Title Only Author and Title

Zhang, X., Singh, J., Li, D., and Qu, F. (2012). Temperature-dependent survival of Turnip crinkle virus-infected Arabidopsis plants relies on an RNA silencing-based defense that requires dcl2, AGO2, and HEN1. J. Virol. 86: 6847-6854.
Pubmed: Author and Title
CrossRef: Author and Title
Google Scholar: Author Only Title Only Author and Title

Zhou, Y., Ryabov, E., Zhang, X., and Hong, Y. (2008). Influence of viral genes on the cell-to-cell spread of RNA silencing. J. Exp. Bot. 59: 2803-2813.
Pubmed: Author and Title
CrossRef: Author and Title
Google Scholar: Author Only Title Only Author and Title